

Abrasive-assisted Nickel Electroforming Process with Moving Cathode

Jianhua REN¹ · Zengwei ZHU¹ · Chunqiu XIA¹ · Ningsong QU¹ · Di ZHU¹

Received: 12 May 2016/Revised: 16 December 2016/Accepted: 5 January 2017/Published online: 17 March 2017
© Chinese Mechanical Engineering Society and Springer-Verlag Berlin Heidelberg 2017

Abstract In traditional electroforming process for revolving parts with complex profiles, the drawbacks on surface of deposits, such as pinholes and nodules, will lead to varying physical and mechanical properties on different parts of electroformed components. To solve the problem, compositely moving cathode is employed in abrasive-assisted electroforming of revolving parts with complicated profiles. The cathode translates and rotates simultaneously to achieve uniform friction effect on deposits without drawbacks. The influences of current density and translation speed on the microstructure and properties of the electroformed nickel layers are investigated. It is found that abrasive-assisted electroforming with compound cathode motion can effectively remove the pinholes and nodules, positively affect the crystal nucleation, and refine the grains of layer. The increase of current density will lead to coarse microstructure and lower micro hardness, from 325 HV down to 189 HV. While, faster translational linear speed produces better surface quality and higher micro hardness, from 236 HV up to 283 HV. The weld-ability of the electroformed layers are also studied through the metallurgical analysis of welded joints between nickel layer and 304 stainless steel. The electrodeposited nickel layer shows fine performance in welding. The novel compound

motion of cathode promotes the mechanical properties and refines the microstructure of deposited layer.

Keywords Nickel electroforming · Abrasive · Compound motion · Weldability

1 Introduction

Electroforming is a precision manufacturing technology in which metal ions are deposited on a cathode's surface to manufacture the parts. Layer depositing on the cathode can copy microscopic detail, reproduce accurate dimensions, and form components of controllable material property [1–5]. Nickel is considered as one of the most important metals in electroforming for its excellent mechanical, physical and chemical properties. Electroformed nickel has so many desirable functions that it is widely used in applications such as precision mould, shaped charge liner, cryogenic upper stage main engine, and micro-nano manufacturing technology [6–9], etc.

However, the applications of traditional electroforming process always go with some drawbacks in the coating, for example, pinholes and nodules on the surface, coarse grain size and long electroforming cycle [10, 11].

So far, a majority of researchers were engaged in various kinds of additives, some of which could really reduce the grain size and enhance the strength of the deposits in electroforming process, others could eliminate the pits and obtain smooth coating [12, 13]. Yet, it is difficult to maintain the electrolyte baths because the additive agents were consumed during the electrodeposited process by either decomposition or being absorbed on the cathode which is leading to codeposition of sulfur and carbon [14, 15]. Researchers have blamed the high-temperature

Supported by National Natural Science Foundation of China (Grant No. 51475239) and Program for New Century Excellent Talents in University of China (Grand No. NCET-10-0074).

✉ Zengwei ZHU
zhuzw@nuaa.edu.cn

¹ College of Mechanical and Electrical Engineering, Nanjing University of Aeronautics and Astronautics, Nanjing 210016, China

ductility losses in nickel on sulfur and carbon that are supposed to give rise to the embrittlement of deposits [16].

In addition, there are still many methods developed by researchers to solve the problem. As reported by TIAN, et al [17], a frictional jet electrodeposition process was developed to manufacture nickel parts with complicated shape and smooth surface. ZHAO, et al [18], developed a device of selective electro-deposition rapid prototyping with electrolyte jet, and obtained deposited layer with nano-crystalline. LEI, et al [19], researched high frequency pulse current and strong electrolyte flushing method and electrodeposited nanocrystalline nickel with fine deposited layer surface quality and high tensile strength. Ultrasound was also employed in electroforming process to improve the performance and surface quality of deposits [20]. However, the attempts mentioned above for electroforming always depended on complex facilities which were too expensive.

Studies made by researchers have shown that abrasive-polishing-assisted nickel electroforming process could eliminate pinholes, remove the nodules, and thus near-mirror electroformed layer is obtained without any organic additives [11]. It is also reported that pure rotational motion can supply uniform friction effect in simple cylindrical mandrel abrasive-assisted nickel electroforming process [10, 11]. Furthermore, taking complex shaped non-rotating parts into consideration, a designed translational cathode is carried out in process [21, 22]. However, for revolving parts of complicated profiles in abrasive-assisted nickel electroforming process, there are different circular velocities along the axial direction of cathode because of diverse curvature radius for single rotational motion. Besides, the varying electric field intensity on cathode surface for single translational motion have limitations in electroforming process. The friction effect can not achieve consistent surface of deposit layer by single cathode motion, which will result in the variation of mechanical, physical properties and morphology microstructure of deposited layer along the axial direction. To solve this problem, a complicatedly moving cathode with combination of translation and rotation was proposed in abrasive-assisted electroforming process.

In this paper, a cathode of compound movement containing translational and rotational motion, which was supposed to achieve uniform friction effect on deposits of revolving parts with complicated surface, was employed to obtain nickel layer for the abrasive-assisted electroforming. Combining moving cathode's translation with rotation, the free ceramic beads were employed to polish the surface slightly and uniformly in a complicated way which could effectively remove the pinholes and nodules, positively affect the crystal nucleation, and refine the grains of layer. The schematic view of mechanism of electroforming

process with moving cathode was shown in Fig. 1 and Fig. 2. Homogeneous and smooth electroformed layer was achieved. The influences of current density and translation speed on the microstructure and properties of electroformed nickel layers were investigated.

2 Experimental Procedures

Figure 1 illustrates the schematic diagram of the experimental apparatus. The cathode's translational movement is carried out by a planar worktable as charged object by stepper motor in X/Y axis linkage. And a speed control motor was employed to drive the rotation of the cathode via transmission mechanism. The rotational speed of the mandrel was set to a fixed value. Nickel pellets were used as anode. A stainless steel cylinder mandrel was used as cathode in horizontal type whose deposit area was $\varphi 70 \text{ mm} \times 100 \text{ mm}$. Free ceramic beads in 0.8–1.2 mm diameter were chosen as the abrasive medium filling the space between the electrodes to maintain continuous friction on the cathode's surface in the process of electroforming. The electrolyte is pumped from the storage bath to the electroforming unit and flows through the gap between cathode and anode. Both the electrolyte flushing and the moving cathode motion served as the agitation of the electrolyte. The electrolyte's temperature is controlled

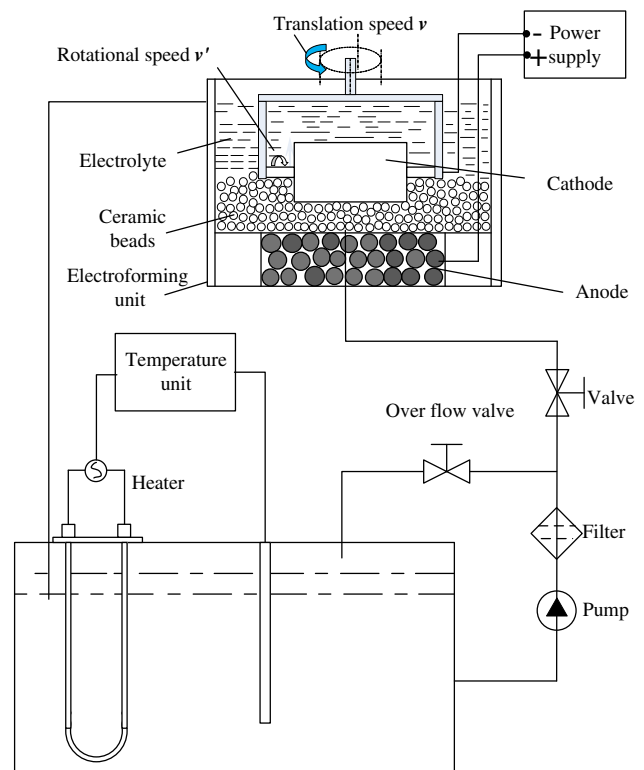


Fig. 1 Schematic diagram of experimental apparatus

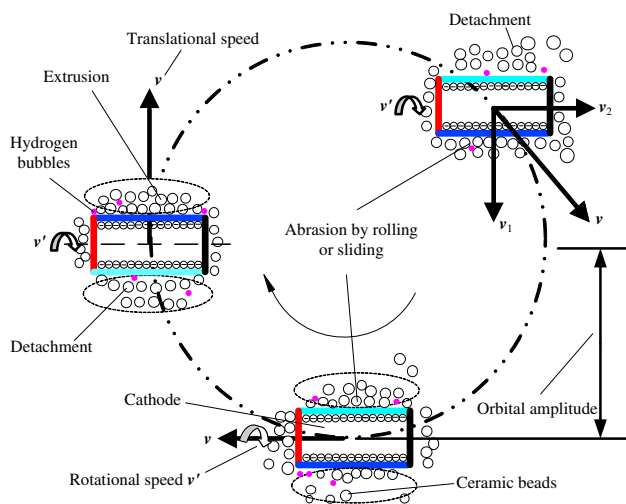


Fig. 2 Schematic top view of mechanism of electroforming process with moving cathode under perturbing of ceramic beads

by a heater and temperature controller. Before deposition, the cathode was mechanically polished, degreased with organic solvent, and rinsed with ethanol.

All solutions were prepared by deionized water and analytical reagents were used. No additives were used. The solution content and the experiment condition are shown in Table 1. At the end of the process, the cathode was immediately withdrawn, rinsed with deionized water, dried and then detected.

A HITACHI S3400N SEM was used to observe the surface morphology of the samples. A HXS-1000A Vickers micro hardness tester was used to detect the micro hardness of the nickel deposits at room temperature. A load of 0.49 N was applied and kept for 15 s. The final value quoted for the hardness of each deposit is the average of six times. The metallurgical analysis of welded joints was performed at room temperature using a MR5000 metallographic microscope.

In welding, a HG-Z99S2 type dye penetrant flaw detection agent was used. The welding joint was scrubbed by the metal cleaner with a clean dry cloth, then the penetrant agent was sprayed on the surface of the joint by a distance of 20–30 mm, the joint surface must be

Table 1 Bath composition and process conditions of nickel electroforming

Electrolyte and process conditions	Quantity
$\text{Ni}(\text{NH}_2 \cdot \text{SO}_3)_2 \cdot 6\text{H}_2\text{O} / (\text{g} \cdot \text{L}^{-1})$	400
$\text{H}_3\text{BO}_3 / (\text{g} \cdot \text{L}^{-1})$	30
$\text{NiCl}_2 / (\text{g} \cdot \text{L}^{-1})$	15
PH	4.0–4.5
Temperature / °C	43±2
Current density / ($\text{A} \cdot \text{dm}^{-2}$)	1–6

completely covered for 10 min at room temperature. Excess penetrant should be wiped down and the joint was scrubbed by the metal cleaner with a clean dry cloth again. Then the developer would be sprayed onto the joint surface, a few minutes later, to see whether there were red marks came out.

3 Analysis of Friction Mechanism

Figure 2 shows the schematic top view of mechanism of electroforming process with moving cathode under perturbing of ceramic beads. Significantly, a moving cathode will achieve consistent friction effect for revolving parts of complicated profiles which would result in the uniformity of the mechanical, physical property and morphology microstructure along the axial direction. For the ceramic beads didn't completely cover the cathode, on one hand, the cathode rotation could achieve uniform polishing effect at height divisions, maintain the surface in same electric field intensity, and make the current density distribution even; On the other hand, there are same circular velocities on different parts of the cathode with the cathode translation making sure the polishing effect on the whole surface in uniformity. The cathode movement combines translation and rotation. When the cathode moved, the rotation was set at low speed, while the translation speed was much higher and acted the key role in driving the beads. Indeed, the trajectory of translation was designed in line with the cathode shapes, such as square and circle. It's well known that the generation of hydrogen bubbles is inevitable in nickel electroforming process. However, the hydrogen adsorption resistance of free beads polishing has been proved by a lot researches [11, 22].

The ceramic beads driven by both the moving cathode and the electrolyte flushing actually act as the agitation of the electrolyte. The rate of mass transfer, the slowest one of the three main steps run through a metal electrodeposition process [22], was believed to be speeded up by the complicate movement of hard ceramic beads. So the electrodeposition rate was improved.

Given the fact that the micro-profile of a seed layer surface is far from ideally smooth, there are micro-recesses and micro-peaks on the mandrel. Current density distribution on the cathode surface decreases from a micro-peak into a micro-depression. So analysis about the micro leveling mechanism of ceramic beads is necessary. The cathode metal deposit is thicker on the micro peaks than the microgrooves. As electroforming process in progress, the surface of the deposit would go rougher, and a lot more time would be spent on the recesses to obtain required thickness. As can be seen from Fig. 3, the micro-leveling action of ceramic beads is presented during the

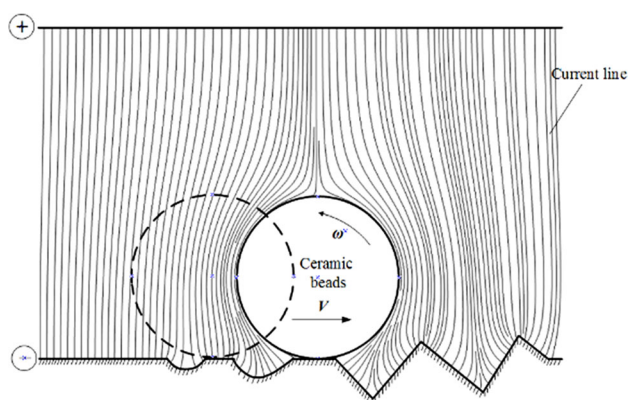


Fig. 3 Schematic view of micro leveling action of ceramic beads

electrodeposition process. The dynamical ceramic beads polish the micro-peaks and renovate the discharged ions close-by. Most importantly, the nonconductive ceramic beads shield the micro flat produced by the ceramic beads' grinding action on the micro-peaks, relatively increase the current density in the micro-recesses. Correspondingly, the growth of the micro-peak is inhibited and the depression growth promoted. The shielding effect of ceramics will work with beads diameter in proper size experimentally [23]. On the one hand, smaller sized beads get coacervated into a paste and prevent the electrodeposition reaction; on the other hand, bigger ones will leave deep grinding marks. As a result, smooth surface deposit layer with decreased groove depth and rounded groove edges was fabricated.

4 Results and Discussion

4.1 Surface Morphology

As can be seen from Fig. 4, SEM morphologies of electroformed nickel deposits with moving cathode at different translation speed are presented as follows. Figure 4(a), (b) and (c) show the smooth deposits electroformed in bath with ceramic beads, while (d) shows the deposited layer in bath without ceramic beads. Obviously, there are distinct abrasion marks on the deposits from bath with ceramic beads and the granular structure is smaller on the deposit than that from bath without beads. Moreover, as translation speed increases, the abrasion marks become more distinguishable and grains grow smaller. The results imply that faster translational linear speed produced better surface quality. There is a strong correlation between ceramic beads polishing effect and the grain size. For complex shaped mandrel, maybe it follows that the more complicated the designed cathode movement is, the better friction effect will be.

Figure 5 shows SEM morphologies of abrasive-assisted electroformed nickel with moving cathode at different

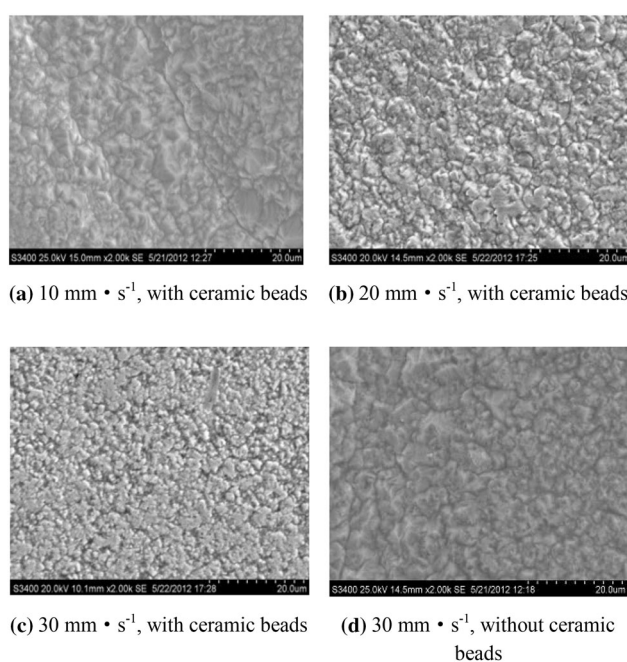


Fig. 4 SEM morphologies of electroformed nickel with moving cathode at different translation speed, current density 3 A dm^{-2}

current density. Associating with Fig. 4, similar tendency also goes for the effect of current density. When the current density increases, the marks can only be seen at local area smaller by smaller and the grains grow bigger. As a result, the abrasion mark is non-distinguishable and the grains become coarser at the same translational linear speed with increasing current density. The abrasion effect driven by cathode with confirmed translational speed at $20\text{ mm}\cdot\text{s}^{-1}$

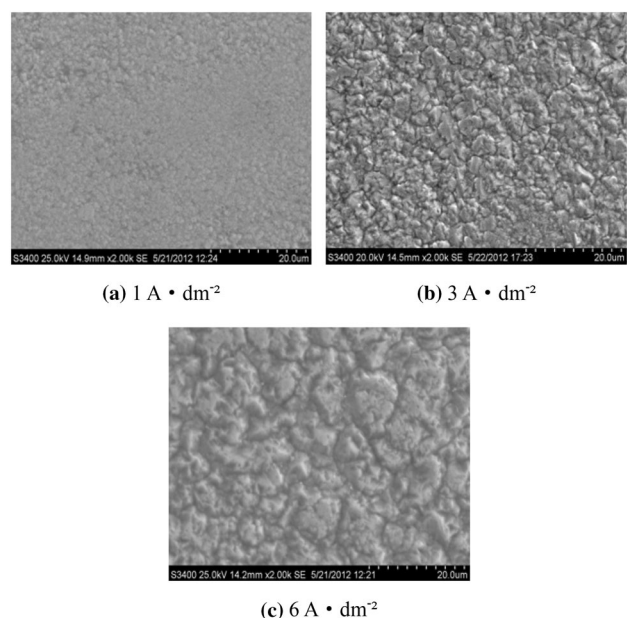


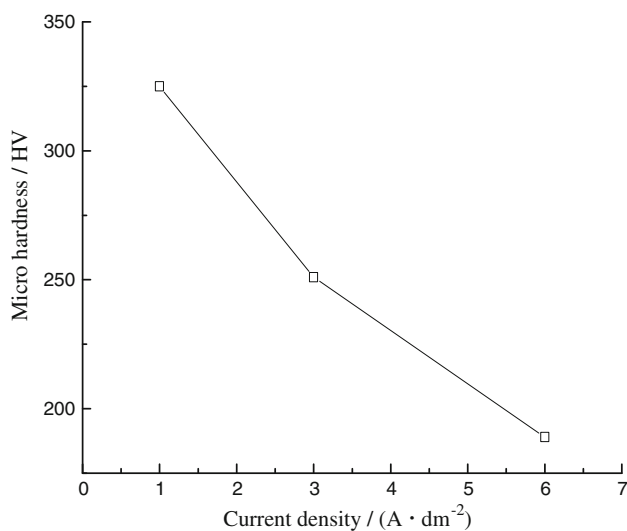
Fig. 5 SEM morphologies of electroformed nickel with moving cathode at different current density, translation speed 20 mm s^{-1}

can't compensate the degree of coarse grains grow produced by increasing current density.

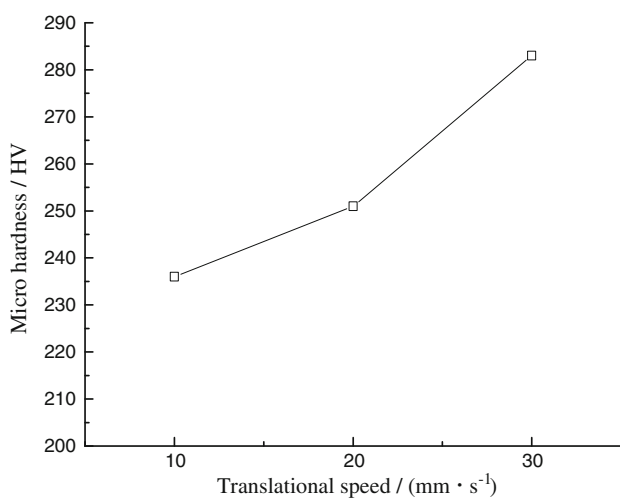
The SEM morphology pictures illustrate that the free abrasives can polish the surface of the deposits and increase activated points on the cathode surface, which was beneficial to refine grains and improve the morphology. However, the increasing of the current density will make the grain grow bigger and weaken the free abrasive polishing effects.

4.2 Variation of Micro Hardness

Effects of current density and translational speed on hardness of electroformed nickel with moving cathode from bath with ceramic beads are shown in Fig. 6. The



(a) Translational speed $20 \text{ mm} \cdot \text{s}^{-1}$



(b) Current density $3 \text{ A} \cdot \text{dm}^2$

Fig. 6 Effects of current density and translational speed on hardness of electroformed nickel with moving cathode

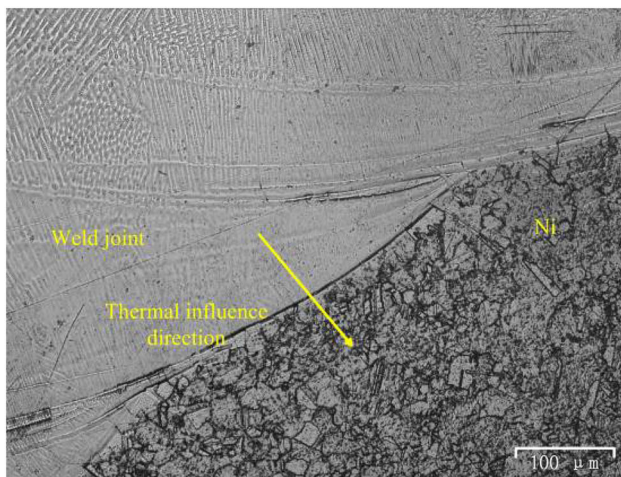
micro hardness value of deposit from bath with ceramic beads at different current density is between 189 HV and 325 HV. When current density increases from $1 \text{ A} \cdot \text{dm}^{-2}$ to $6 \text{ A} \cdot \text{dm}^{-2}$, the micro hardness value sharply decreases. Figure 6(a) is shown below to have a negative correlation between current density and micro hardness. Higher current density may lead to coarser crystal grains and the loose structure reflected by low micro hardness value. However, Fig. 6(b) shows the relationship between translation speeds and hardness from bath with ceramic beads. A positive correlation can easily be found out. The micro hardness value rises along with the increasing translation speed. It may be concluded that ceramic beads driven by translational and rotational cathode can polish and impact the complicated cathode surface, achieving compact deposit structure with small grain size, and combining cathode movement is supposed to have uniform abrasion effect on revolving parts with complicated profiles. The polishing can increase the activated points and refine grain size, which can obtain higher micro hardness according to the Hall-Petch theory [22]. Unlike the current effect does, the hardness rises not so prominently with increasing translational speed, because the increasing of current density was observed to weaken the polishing effect of free abrasives, which led to the reduction of micro hardness by coarse grain.

4.3 Weldability

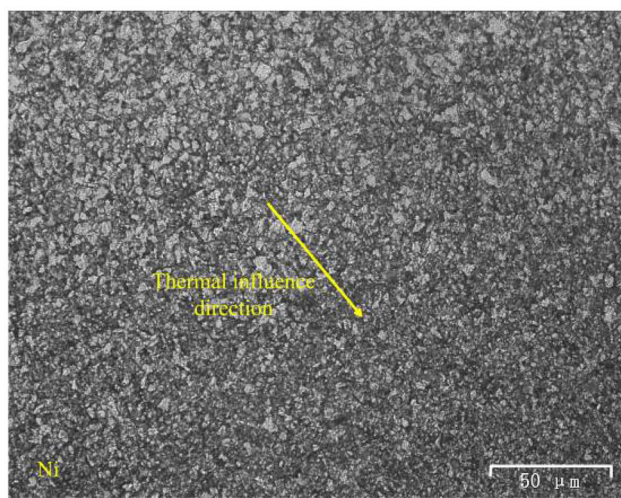
Figure 7 shows the photo of a welding test sample produced by using manual tungsten argon arc welding. A 2 mm thick or more nickel layer was obtained with moving cathode in abrasive-assisted electroforming process. The welding joint between nickel layer and 304 stainless steel was under dye penetrant inspection to find out if there are crack or excessive porosity defects in it with a dye penetrant flaw detection agent. Subsequently, if there was red



Fig. 7 Photo of welding test sample



(a) Area near weld line



(b) Magnification of heat affected area in nickel

Fig. 8 Metallographic structure of weld joint of electroformed nickel with 304 stainless steel

marks came out, cracks or porosity in the welding joint would be found out; Conversely, if there was no red marks, electroformed nickel, 304 stainless steel and the welding joint would be entire one. The welding current is 110–120 A. As can be seen clearly, there is all white developer on the welding joint surface without any red penetrant. So the 304 stainless steel was successfully welded to the electroformed nickel.

DINI, et al [14, 16], revealed a loss of high-temperature ductility of electroformed nickel at temperatures above 400 °C. Even worse, at high welding temperature, some had experienced difficulties such as cracking or excessive porosity in welding this material at one time or another, due to the presence of trace amounts of impurities co-deposited in the layer [15, 24]. The loose structure with pits and pinholes, hydrogen bubbles and impurities such as C and S precipitated in grain boundary will do harm to the

weld joint of electroformed nickel leading to weld cracks [25]. While the outer surface of the test sample was in good condition, the metallurgical analysis [26] of welded joints of 304 stainless steel and nickel deposit with moving cathode from bath with ceramic beads was studied to find out whether there were micro cracks in it, as shown in Fig. 8 below. Figure 8(a) and (b) exhibit the cross-section perpendicular to the welding direction, and the arrows in the picture show the direction away from heat affected area. The pictures show that the nickel crystal grains get bigger and bigger gradually near by the joint, but there is no crack or porosity. So the metallurgical pictures imply that the nickel layer with smooth surface, fine grains and compact structure owes to ceramic beads polishing which can prevent hydrogen bubbles from adhering, increase the activated points and refine crystal grains, and it was effective to prevent the grains from getting too big to be welded. Moreover, the additive-free electroformed process with ceramic beads cut down the precipitation of S from grain boundary. As a result, no porosity or heat cracking was found. The two points mentioned above will promote compact structure of electrodeposited nickel layer showing fine performance in welding.

5 Conclusions

- (1) The free ceramic beads driven by compound cathode motion can effectively remove the pinholes and nodules, positively affect the crystal nucleation, and refine the grains of layer in uniformity.
- (2) The increase of current density leads to coarse microstructure and lower micro hardness. While, faster translational linear speed produces better surface quality and higher micro hardness.
- (3) The metallurgical analysis of welded joints of 304 stainless steel and nickel deposit with cathode of compound motion under perturbation of ceramic beads is studied. 2 mm thick or more nickel layer with smooth surface and compact structure is obtained and the electrodeposited nickel layer shows fine performance in welding.

References

1. BROUSSEAU E B, DIMOV S.S., PHAM D T. Some recent advances in multi-material micro- and nano-manufacturing[J]. *The International Journal of Advanced Manufacturing Technology*, 2010, 47(1–4): 161–180.
2. QU Ningsong, QIAN Wanghuan, HU Xiaoyun, et al. Preparation of a microprism Ni-CeO₂ nanocomposite mold by electroforming[J]. *Materials & Manufacturing Processes*, 2014, volume 29(1): 37–41.

3. HUANG MingShyan, KU HongHua. Microinjection molding of light-guided plates using LIGA-like fabricated stampers[J]. *Journal of Applied Polymer Science*, 2011, 122(5): 3446–3455.
 4. LARSON C, SMITH J R. Recent trends in metal alloy electrolytic and electroless plating research: a review[J]. *Transactions of the IMF*, 2011, 89(6): 333–341.
 5. ZHONG Z W. Recent advances in polishing of advanced materials[J]. *Materials and Manufacturing Processes*, 2008, 23(5): 449–456.
 6. MING Pingmei, ZHU Di, HU Yangyang, et al. Numerical analysis on mass transport in micro electroforming of micro structures with high-aspect-ratio[J]. *Chinese Journal of Mechanical Engineering*, 2008, 44(8): 195–201. (in Chinese).
 7. QIAN Jiangang, LI Haiting, LI Pengrui. Effect of technology parameters on microstructure and properties of electroforming nickel layer[J]. *Rare Metal Materials and Engineering*, 2015, 44(7): 1758–1762. (in Chinese).
 8. WENG Can, ZHOU Mingyong, JIANG Bingyan, et al. Improvement on replication quality of electroformed nickel mold inserts with micro/nano-structures[J]. *International Communications in Heat & Mass Transfer*, 2016, 75: 92–99.
 9. LIU Gang, TIAN Yangchao. Research and application of LIGA process at national synchrotron radiation laboratory[J]. *Chinese Journal of Mechanical Engineering*, 2008, 44(11): 47–52. (in Chinese).
 10. ZHU Zengwei, ZHU Di, QU Ningsong. Effects of simultaneous polishing on electrodeposited nanocrystalline nickel[J]. *Materials Science and Engineering: A*, 2011, 528 (24): 7461–7464.
 11. ZHU Di, ZHU Zengwei, QU Ningsong: Abrasive polishing assisted nickel electroforming process[J]. *CIRP Annals Manufacturing Technology*, 2006, 55(7): 193–196.
 12. MIMANI T, MAYANNA S M, MUNICHANDRAIAH N. Influence of additives on the electrodeposition of nickel from a Watts bath: a cyclic voltammetric study[J]. *Journal of Applied Electrochemistry*, 1993, 23(4): 339–345.
 13. OLIVEIRA E M, FINAZZI G A, CARLOS I A. Influence of glycerol, mannitol and sorbitol on electrodeposition of nickel from a Watts bath and on the nickel film morphology[J]. *Surface and Coatings Technology*, 2006, 200(20): 5978–5985.
 14. DINI J W, JOHNSON H R, SAXTON H J. Influence of sulfur content on the impact strength of electroformed nickel[J]. *Electrodeposition and Surface Treatment*, 1974, 2(3): 165–176.
 15. BROOKS J A, DINI J W, JOHNSON H R. Effects of impurities on the weldability of electroformed nickel[J]. *SAND 78–8774, US Sandia Laboratories*, 1978.
 16. DINI J W, JOHNSON H R. High-temperature ductility of electro-deposited nickel[J]. *Sandia Laboratories SAND 77–8020*, July, 1977.
 17. TIAN Zongjun, WANG Gguifeng, HUANG Yinhui, et al. Rapid prototyping of nickel metal products via jet electrodeposition[J]. *Huanan Ligong Daxue Xuebao/Journal of South China University of Technology*, 2010, 38(12): 41–44. (in Chinese).
 18. ZHAO Jianfeng, HUANG Yinhui, WU Ande. Fundamental experimental study on selective electrodeposition rapid prototyping with electrolyte jet[J]. *Chinese Journal of Mechanical Engineering*, 2003, 39(4): 75–78. (in Chinese).
 19. LEI Weining, ZHU Di, QU Ningsong. Research on mechanical properties of nanocrystalline electroforming layer[J]. *Chinese Journal of Mechanical Engineering*, 2004, 40(12): 124–127. (in Chinese).
 20. XUE Yujun, LIU Hongbin, LAN Mingming, et al. High temperature oxidation resistance of Ni-CeO₂ nanocomposite coatings by pulse electrodeposition under ultrasound condition[J]. *Zhongguo Youse Jinshu Xuebao/Chinese Journal of Nonferrous Metals*, 2010, 20(8): 1599–1604. (in Chinese).
 21. ZHU Zengwei, WANG Dong, REN Jianhua. Abrasive-assisted electroforming of nickel on translational cathode[C]//*Materials Science Forum. Trans Tech Publications*, 2014, 770: 145–149.
 22. LI Xuelei, ZHU Zengwei, ZHU Di, et al. Orbital-abrasion-assisted electroforming of non-rotating parts[J]. *Journal of Wuhan University of Technology-Mater*, 2011, 26(5): 827–831.
 23. LI Xuelei., ZHU Di, ZHU Zengwei. Effect of free particles to the abrasion-assisted electroforming technique[J]. *Electromachining & Mould*, 2010: 35–39. (in Chinese).
 24. BROOKS J A, DINI J W, JOHNSON H R. Causes of weld porosity in electroformed nickel[J]. *Metal Finishing*, 1981, 75(5): 41–45.
 25. LU Anli, REN Jialie., LU Baocai, et al. The investigation on welding cracks of electroformed nickel of aero-space components[J]. *Missiles & Space Vehicles*, 1993,3: 65–74. (in Chinese).
 26. ZHANG, Ling, MIN Junying, WANG bin, et al. Constitutive model of friction stir weld with consideration of its inhomogeneous mechanical properties[J]. *Chinese Journal of Mechanical Engineering*, 2016, 29(2):357–364.
- Jianhua REN** born in 1986, is currently a PhD candidate at *College of Mechanical and Electrical Engineering, Nanjing University of Aeronautics and Astronautics, China*. His research interests include electroforming and electrochemical machining. Tel: +86-25-84895912; E-mail: renjianrun@163.com
- Zengwei ZHU** born in 1971, is currently a professor at *Nanjing University of Aeronautics and Astronautics, China*. His research interests include electrochemical machining, electroforming, and micro-electrochemical machining. Tel: +86-25-84896605; E-mail:zhuzw@nuaa.edu.cn
- Chunqiu XIA** born in 1989, is currently a master candidate at *Nanjing University of Aeronautics and Astronautics, China*. His current research interests is electroforming. E-mail:xcqchina@163.com
- Ningsong QU** born in 1968, is currently a professor and PhD supervisor at *College of Mechanical and Electrical Engineering, Nanjing University of Aeronautics and Astronautics, China*. He received the Ph.D. degree from the same university. His current research interests are electrochemical machining, electroforming, and microelectrochemical machining. E-mail:nsqu@nuaa.edu.cn
- Di ZHU** born in 1954, is currently a professor at *Nanjing University of Aeronautics and Astronautics, China*. His research interests include electrochemical machining, electroforming, and micro-electrochemical machining. Tel: +86-25-84896866; E-mail: dzhu@nuaa.edu.cn